JOURNAL OF BACTERIOLOGY, May 1995, p. 2804–2812 Vol. 177, No. 10
0021-9193/95/$04.00+0

Biochemical Characterization of *gapB*-Encoded Erythrose 4-Phosphate Dehydrogenase of *Escherichia coli* K-12 and Its Possible Role in Pyridoxal 5′-Phosphate Biosynthesis

GENSHI ZHAO, ANDREW J. PEASE, NIPALI BHARANI, AND MALCOLM E. WINKLER*

Department of Microbiology and Molecular Genetics, University of Texas Houston Medical School, Houston, Texas 77030

Received 26 January 1995/Accepted 16 March 1995

One step in de novo pyridoxine (vitamin B_6) and pyridoxal 5′-phosphate biosynthesis was predicted to be an oxidation catalyzed by an unidentified D-erythrose-4-phosphate dehydrogenase (E4PDH). To help identify this E4PDH, we purified the *Escherichia coli* K-12 *gapA*- and *gapB*-encoded dehydrogenases to homogeneity and tested whether either uses D-erythrose-4-phosphate (E4P) as a substrate. *gapA* (*gap1*) encodes the major D-glyceraldehyde-3-phosphate dehydrogenase (GA3PDH). The function of *gapB* (*gap2*) is unknown, although it was suggested that *gapB* encodes a second form of GA3PDH or is a cryptic gene. We found that the *gapB*-encoded enzyme is indeed an E4PDH and not a second GA3PDH, whereas *gapA*-encoded GA3PDH used E4P poorly, if at all, as a substrate under the in vitro reaction conditions used in this study. The amino terminus of purified E4PDH matched the sequence predicted from the *gapB* DNA sequence. Purified E4PDH was a heat-stable tetramer with a native molecular mass of 132 kDa. E4PDH had an apparent K_m value for E4P [K_m^{app}(E4P)] of 0.96 mM, an apparent k_{cat} catalytic constant for E4P [k_{cat}^{app}(E4P)] of 200 s^{-1}, K_m^{app}(NAD^+) of 0.074 mM, and k_{cat}^{app}(NAD^+) of 169 s^{-1} in steady-state reactions in which NADH formation was determined. From specific activities in crude extracts, we estimated that there are at least 940 E4PDH tetramer molecules per bacterium growing in minimal salts medium plus glucose at 37°C. Thin-layer chromatography confirmed that the product of the E4PDH reaction was likely the aldonic acid 4-phosphoerythronate. To establish a possible role of E4PDH in pyridoxal 5′-phosphate biosynthesis, we showed that 4-phosphoerythronate is a likely substrate for the 2-hydroxy-acid dehydrogenase encoded by the *pdxB* gene. Implications of these findings in the evolution of GA3PDHs are also discussed. On the basis of these results, we propose renaming *gapB* as *epd* (for D-erythrose-4-phosphate dehydrogenase).

Pyridoxine 5′-phosphate (PNP) is a direct precursor of the ubiquitous, essential coenzyme, pyridoxal 5′-phosphate (PLP) (Fig. 1) (4, 14, 15). PNP is synthesized in *Escherichia coli* K-12 by a convergent, branched pathway (Fig. 1) (14, 15, 29, 38–40, 46, 48). One branch of the pathway leads from the important common intermediate, D-erythrose-4-phosphate (E4P), to 4-phospho-hydroxy-L-threonine (4PHT) or its dephosphorylated form, 4-hydroxy-L-threonine (4HT) (15, 19, 39, 58). Presently, it is not known which form of 4HT is used as an obligatory intermediate. According to this scheme, 4PHT or 4HT is condensed with 1-deoxy-D-xylulose to give PNP or pyridoxine (PN), respectively, as the first B_6-vitamer synthesized. Two oxidations and one transamination are required to convert E4P into 4PHT (Fig. 1). The oxidation of the aldonic acid 4-phosphoerythronate (4PE) and the subsequent transamination are thought to be catalyzed sequentially by the enzymes encoded by the *pdxB* and *serC*(*pdxF*) genes, respectively (Fig. 1) (14, 15, 39, 43, 48). The remaining dehydrogenase, which converts E4P to 4PE, has not been identified.

Previously, we demonstrated that a NAD^+- or $NADP^+$-dependent E4P dehydrogenase (E4PDH) activity was present in crude extracts of *E. coli* K-12 cells (39). Several observations led us to postulate that *E. coli gapB* may encode this E4PDH activity. *gapB* was first identified as an open reading frame next to *pgk*, which encodes the important glycolytic enzyme 3-phosphoglycerate kinase (1, 22, 33, 34). The amino acid sequence predicted for the putative polypeptide encoded by *gapB* was 41% identical to that of glyceraldehyde 3-phosphate dehydrogenase (GA3PDH), which is encoded by *gapA* (8, 9, 22, 30, 33, 34). Although the *gapA* and *gapB* gene products are evolutionarily related (1, 17, 41), it was never established that *gapB* encodes a second GA3PDH (1). Strikingly, extracts of *gapA* mutants did not contain residual GA3PDH activity indicative of a second active *gap* gene (30, 33, 34). Therefore, it seemed plausible that the *gapB*-encoded dehydrogenase was not a second GA3PDH but instead used a substrate structurally related to glyceraldehyde 3-phosphate (GA3P). The structures of E4P and GA3P are similar and differ by only a single CHOH group. Finally, early work suggested that mammalian GA3PDH utilized E4P as a substrate at a low rate (36, 45). This observation implied that an E4PDH, if present, might be structurally related to GA3PDH.

In this paper, we report the purification and enzymological characterization of the *gapB*-encoded dehydrogenase. Our results confirm the hypothesis that the *gapB*-encoded enzyme is an E4PDH, rather than a second GA3PDH. We also present results consistent with the idea that this E4PDH plays a role in the de novo biosynthesis of the PLP coenzyme.

* Corresponding author. Mailing address: Department of Microbiology and Molecular Genetics, University of Texas Houston Medical School, 6431 Fannin, JFB 1.765, Houston, TX 77030-1501. Phone: (713) 794-1744, ext. 1526. Fax: (713) 794-1782. Electronic mail address: mwinkler@utmmg.med.uth.tmc.edu.

MATERIALS AND METHODS

Materials. D-Isomers of phosphate-sugar compounds (E4P [67%], GA3P [>95%], D-glucose-6-phosphate [G6P; 98%], D-arabinose-5-phosphate [98%], D-ribose-5-phosphate [99%], and D-erythrose [≈50%]), cofactors, coenzymes, reducing agents, arsenate, nucleotide mono- and triphosphates, and molecular

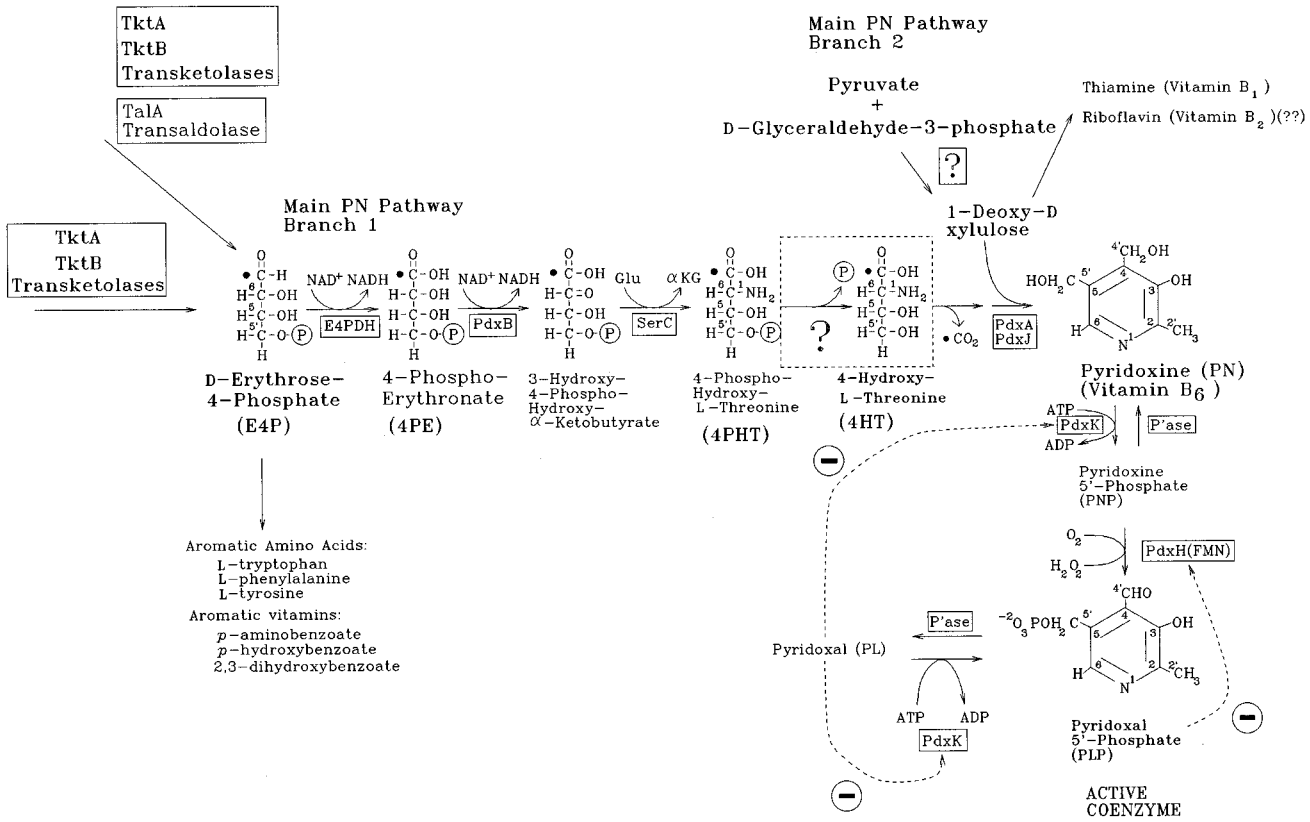

FIG. 1. Proposed PLP biosynthetic pathway showing the two convergent branches leading from E4P and 1-deoxy-D-xylulose to PN (vitamin B_6) and then sequentially from PNP to the active coenzyme, PLP. The boxed reaction may not occur (see Introduction), in which case PNP would be the first B_6-vitamer formed with a complete pyridine ring and the PdxK kinase would not be required in the de novo pathway. The first step of this scheme requires an E4PDH activity to convert E4P into 4PE. Points of negative feedback control are indicated by circled minus signs. Numbering refers to the pyridine ring of PN, and the black dot marks a carbon lost during ring closure. Alternate names for compounds: 4HT, 3-hydroxyhomoserine; 1-deoxy-D-xylulose, D-1-deoxyxylulose or 1-deoxy-D-*threo*-pentulose. For additional details about the pathway, see the text.

weight standards for gel filtration (cytochrome *c* [12.4 kDa], carbonic anhydrase [29 kDa], bovine serum albumin [BSA; 66 kDa], and alcohol dehydrogenase [150 kDa]) were purchased from Sigma Chemical Co. (St. Louis, Mo.). PNP was synthesized by reducing PLP with sodium borohydride as described previously (59). 4PE was synthesized from E4P by bromine oxidation as previously described (31, 35). 4HT was generously provided by I. D. Spenser (McMaster University, Ontario, Canada). Hydroxyapatite and molecular weight standards for sodium dodecyl sulfate-polyacrylamide gel electrophoresis (SDS-PAGE) were from Bio-Rad Laboratories (Hercules, Calif.). DEAE-cellulose was obtained from Whatman, Inc. 5′-AMP–Sepharose-affinity resin was purchased from Pharmacia LKB Biotechnology (Alameda, Calif.). Nucleotide triphosphates and Vent DNA polymerase (*exo*$^+$) for PCR were obtained from New England Biolabs, Inc. (Beverly, Mass.). Restriction endonucleases and other enzymes were purchased from New England Biolabs and Promega Corp. (Madison, Wis.). $P_{T7\text{-}lacO}$–His-6 tag expression vector pET15b and T7 RNA polymerase phage λDE3 were obtained from Novagen, Inc. (Madison, Wis.). G6P dehydrogenase (G6PDH) was purchased from Boehringer Mannheim, Inc. (Indianapolis, Ind.).

Bacterial strains and culture conditions. The following strains of *E. coli* K-12 were used in this study: JM109 [F′ *traD36 lacI*^{q} Δ(*lacZ*)*M15 recA1 endA1 gyrA96 thi hsdR17 supE44 relA1* Δ(*lac-proAB*)] (BRL Life Technologies, Inc., Gaithersburg, Md.), DH5α [F′ *endA1 hsdR17 supE44 thi-1 recA1 gyrA relA* Δ(*lacZYA-argE*)*U169 deoR*] (New England Biolabs), JM109(pUC19), JM109(pTX420 *gapB*$^+$ Ap^r), DH5α(pBR322), DH5α(pTX419 *gapB*$^+$ Ap^r), NU816(W3110 *lacU169 tna-2 sup*^{0}) (C. Yanofsky collection), DF221(*gapA*) (30), and TX3252 [DF221(pTX421 *gapA*$^+$ Cm^r)]. TX2683 [NU426 *pdxB*::Km^r(*Hin*dIII) *serA*::Tn*10*dCamMCS *recA1 srl*::Tn*10*(Tet^r)] was constructed by sequential P1 *vir* phage-mediated generalized transduction of *serA*::Tn*10*dCamMCS (27) and cotransduction of *recA1 srl*::Tn*10* (Tet^r) (32) into NU402 (NU426 *pdxB*::Km^r) (2). TX2687 [TX2683 (λDE3)] was a lysogen carrying the T7 phage RNA polymerase gene under control of the *lac* repressor. TX2691 [TX2687(pTX359 Ap^r)] and TX2730 [TX2687(pTX358 Ap^r)] were used to overexpress His-6–PdxB and His-6–SerC(PdxF) fusion proteins (below).

Luria-Bertani (LB) medium (10 g of NaCl per liter) was prepared from capsules marketed by Bio 101, Inc. (La Jolla, Calif.). Vogel-Bonner (1×E) minimal salts medium containing 0.4% glucose was prepared as described previously (13). Ampicillin (50 μg/ml), chloramphenicol (25 μg/ml), and isopropyl-β-D-thiogalactopyranoside (IPTG, 1 mM) were added to media as indicated.

Cloning *E. coli* K-12 *gapB* (*epd*) and *gapA*. The *gapB* gene, which is renamed *epd* in this report (see Discussion), was PCR amplified from strain NU816 chromosomal DNA by using two primers (5′-CTTCACAAGCTGACAATTT ATTCCAGT and 5′-GGTTAGACAGTTTGTCTTTCAGGTAGT) that flank the published *gapB* promoter and coding sequences (1). The 50-μl PCR reaction mixture contained 0.5 μM (each) primer; 0.3 mM (each) dATP, dCTP, dGTP, and dTTP; 25 ng of NU816 chromosomal DNA, which was purified as described elsewhere (50); 0.6 U of Vent (*exo*$^+$) high-fidelity DNA polymerase; and 1× Vent buffer (New England Biolabs, Inc.). Denaturation at 94°C for 60 s, annealing at 53°C for 60 s, and polymerization at 72°C for 96 s were done for 35 cycles. The amplified PCR product was analyzed by standard agarose gel electrophoresis (47) and digested at internal sites with *Hin*dIII and *Eco*RI restriction endonucleases. The resulting fragments were ligated into *Hin*dIII- and *Eco*RI-cut pBR322 and pUC19 to give plasmids pTX419 and pTX420, which were transformed into strains DH5α and JM109, respectively. Few PCR errors seemed to occur during the high-fidelity PCR amplification, because several separate PCR product fragments gave about the same elevated E4PDH-specific activities when cloned into a given vector (see below). The DNA sequence of the *gapB* coding region from the final isolate of plasmid pTX420, which was the source for E4PDH purification (see below), was determined with an automated Applied Biosystems machine. The amino acid sequence predicted for the pTX420-encoded dehydrogenase was identical to that predicted from the published *gapB* sequence (1).

E. coli gapA was cloned by functional complementation of the *gapA* mutation in strain DF221, which cannot grow on LB or minimal salts medium plus glucose (30). Chromosomal DNA of NU816 (described above) was partially digested with *Sau*3A, and 4- to 10-kb fragments were purified from agarose gels with the Wizard DNA cleanup system (Promega, Inc.). The *Sau*3A DNA fragments were ligated into vector pACYC184, which was digested with *Bam*HI and dephosphorylated with calf intestinal phosphatase (Promega, Inc.). The ligation mixture was

transformed into strain DH5α, which was made competent as described elsewhere (24), and transformants were selected on LB plates containing 25 μg of chloramphenicol per ml. About 15,000 separate transformant colonies were pooled, and plasmid DNA was purified by using the Wizard minipreparation DNA purification system (Promega, Inc.). The resulting NU816 genomic library was transformed into strain DF221 (*gapA*), and transformants were selected on LB plates containing 25 μg of chloramphenicol per ml. After 2 days at 37°C, six transformants appeared on the plates. These transformant colonies were isolated twice on LB plus 25 μg of chloramphenicol per ml and shown to grow on minimal medium plus glucose with chloramphenicol. Extracts were prepared from purified transformants and assayed for GA3PDH activity (below). GA3PDH-specific activity was negligible in the parent DF221 (*gapA*) mutant (data not shown) (30). By contrast, each transformant exhibited GA3PDH-specific activity 5- to 12-fold higher than that of NU816, whose GA3PDH-specific activity was about 0.95 μmol of NADH formed per min per mg of protein. One transformant, designated TX3252, was used as the source for GA3PDH purification (below).

Enzyme assays, kinetics, and analysis of substrates and products. Crude extracts were freshly prepared as described previously (59). The levels of E4PDH and GA3PDH activities were determined by the formation of NADH, which absorbs at 340 nm (molar extinction coefficient, 6,220 M^{-1} cm^{-1}) (12, 45). Reaction mixtures (1 ml) for assaying E4PDH activity contained 50 mM PP_i buffer (pH 8.6), 1 mM dithiothreitol (DTT), 2 mM E4P, 1 mM NAD^+, and 0.1 to 0.5 mg of protein from crude extracts. Reaction mixtures for the determination of GA3PDH activity contained 50 mM PP_i buffer (pH 8.6), 1 mM GA3P, 1 mM NAD^+, 0 or 30 mM arsenate, and 1.0 to 2.0 μg of protein from crude extracts (12, 45). The increase in A_{340} was monitored at 37°C for 3 min for E4PDH and at 30°C for 1.5 min for GA3PDH in a double-beam UV-160 spectrophotometer (Shimadzu Instruments, Inc.). Protein concentrations were determined with the Bradford protein assay kit (Bio-Rad) by using BSA as the standard (7). One unit of E4PDH activity was defined as the formation of 1 nmol of NADH per min at 37°C.

Kinetic analyses of the purified *E. coli* E4PDH were carried out in reaction mixtures (1 ml) containing 50 mM PP_i buffer (pH 8.6), 1 mM DTT, various amounts of NAD^+ or E4P, and 0.05 to 0.5 μg of pure enzyme. Initial velocities were measured by monitoring NADH formation (A_{340}) at 37°C for 2.5 min. Kinetic parameters were determined by fixing one substrate concentration at saturation (NAD^+ = 2 mM, or E4P = 10 mM) while varying the concentration of the other substrate (49a). GA3PDH and E4PDH substrate specificities were determined in reaction mixtures (0.5 ml) containing 50 mM PP_i buffer (pH 8.6), the amounts of the compounds listed in Table 2 (see Results), and 0.5 μg of purified *E. coli* GA3PDH or E4PDH (see below). Increases in A_{340} were monitored at 37°C for 3 min.

Possible inhibition of E4PDH by B_6 vitamers and related compounds was tested in reaction mixtures (1 ml) containing 50 mM PP_i buffer (pH 8.6), 1 mM DTT, 1.2 mM NAD^+, 0.5 mM E4P, 1 μg of purified E4PDH, and 0.1 mM PNP, PN, 4HT, pyridoxal, or PLP. The increase in A_{340} was monitored at 37°C for 3 min. To determine whether nucleotides inhibited E4PDH activity, enzyme assays were performed as described above in reaction mixtures (1 ml) containing 50 mM PP_i buffer (pH 8.6), 1 mM DTT, 1 mM E4P, 0.2 mM NAD^+, 1 μg of purified E4PDH, and 2.0 mM cyclic AMP (cAMP), AMP, ADP, or ATP.

Commercially available E4P (67%), which was probably synthesized by lead tetraacetate oxidation of G6P (51), contained low levels of GA3P (≈6% [mol/mol]), G6P (≈3% [mol/mol]), and an unidentified contaminant (≈24% [wt/wt]) that was probably not a phosphate sugar (see Results). Contamination levels of GA3P were estimated enzymologically from the initial rates of the GA3PDH reaction (see above) against standards containing known amounts of GA3P. Contamination levels of G6P were measured by allowing G6PDH reactions (22) to go to completion and determining the amount of NADPH formed (see above). The substrates and products of the E4PDH reaction were also analyzed by thin-layer chromatography (TLC) on Whatman K2F-cellulose plates (250-μm layer; 20 by 20 cm) which were developed in freshly mixed butanol-acetic acid-water (10:3:7) at room temperature (57). Phosphate sugars were located by spraying the TLC plates with the Hanes-Isherwood reagent as described elsewhere (25). PP_i buffer and other components in the enzyme reaction mixtures formed a greenish spot at the origin, which sometimes seemed to interfere with resolution of the reaction products. However, in the majority of runs (four of five), the reaction products were reproducibly resolved.

Purification of *gapB*-encoded E4PDH. A 240-ml overnight culture of JM109 (pTX420) in LB plus 50 μg of ampicillin per ml was inoculated into eight 2-liter flasks, each containing 1 liter of the same medium. Cultures were grown with vigorous shaking at 37°C to stationary phase (130 to 150 Klett [660 nm] units). Cells were harvested by low-speed centrifugation (10 min, 1,000 × *g* at 4°C), washed once with cold 20 mM KPO_4 buffer (pH 7.5)–1 mM DTT (buffer A), and resuspended in 100 ml of the same buffer. All subsequent steps were performed at 4°C. Cells were disrupted by passage through a 20K French pressure cell (Aminco Laboratories, Inc.) at 20,000 lb/in^2. The resulting suspension was centrifuged at 150,000 × *g* for 60 min (Beckman Ti80 rotor). The crude extract supernatant was loaded onto a DEAE-cellulose column (5 by 12 cm) that had been previously equilibrated with buffer A. The column was washed with 750 ml of buffer A and eluted with a linear 0 to 800 mM KCl gradient in buffer A. Eleven 8-ml fractions showing high levels of E4PDH activity were pooled, added to a dialysis bag (8-kDa cutoff; Spectrum Medical Industries, Inc., Houston, Tex.), and dialyzed overnight against 5 liters (no changes) of 20 mM KPO_4 buffer (pH 8.2)–1 mM DTT (buffer B). The sample was applied to a second DEAE-cellulose column (2.5 by 8 cm) equilibrated with buffer B. The column was washed with 200 ml of buffer B and eluted with a linear 0 to 800 mM KCl gradient in buffer B. Twelve 5-ml fractions showing high levels of E4PDH activity were pooled, concentrated to about 5 ml in a medium-size stirred-cell concentrator containing a 50-kDa cutoff membrane (Spectrum Medical Industries, Inc.), and diluted with 20 to 30 ml of 20 mM KPO_4 buffer (pH 7.2)–1 mM DTT (buffer C). Concentration of the sample and change of buffer were repeated one or two more times. The concentrated sample (5 ml) was applied to a hydroxyapatite column (2.5 by 5 cm) equilibrated with buffer C. The column was eluted with 90 ml of buffer C, and 13 4-ml fractions with high levels of E4PDH activity, which was not retained by hydroxyapatite, were pooled and concentrated without a buffer change. Solid NaCl was added to the concentrated sample to a final concentration of 150 mM, and a portion containing 2 mg of protein was applied to a 5′-AMP–Sepharose-affinity column (0.5 by 6 cm; 1 ml) which was equilibrated with 20 mM KPO_4 buffer (pH 7.2)–1 mM DTT–150 mM NaCl (buffer D). The column was washed with 40 ml of buffer D and then eluted with a linear 0 to 12 mM NAD^+ gradient in buffer D. Ten 3-ml fractions showing high levels of E4PDH activity were pooled and concentrated with a change to buffer A. The 5′-AMP–Sepharose column was regenerated by washing with 3 column volumes each of 0.1 M Tris-HCl (pH 8.5)–0.5 M NaCl followed by 0.1 M acetic acid (pH 4.5)–0.5 M NaCl. Washing with the two solutions was repeated two more times, and the column was again equilibrated with buffer D. Another 2 mg of protein from the pooled hydroxyapatite fraction was then applied to the equilibrated 5′-AMP–Sepharose column, which was washed and eluted as described above. The cycle was repeated until all of the pooled hydroxyapatite fraction (23 mg) was purified. Attempts to load more protein onto the affinity column resulted in substantial loss of sample due to nonbinding. A larger affinity column would reduce the number of repetitions necessary to purify the entire sample, but it is prohibitively expensive. The purified preparations from two column runs were pooled and concentrated to about 5 ml with a change to buffer A (above). Glycerol was added to 15% (vol/vol), and the final samples were divided into 0.5-ml aliquots and stored at −75°C. The concentration, buffer change, and storage steps were repeated for the remainder of the purified sample from the affinity column. Samples were thawed only once for experiments and then kept at 4°C.

Two-step purification of *gapA*-encoded GA3PDH. We devised a short protocol for GA3PDH purification different from previously used schemes (12, 51a). A 3.6-liter overnight culture of TX3252 (described above) grown with shaking in LB plus 25 μg of chloramphenicol per ml at 37°C was collected, and the cells were disrupted as described above. The crude extract prepared in buffer B (see above) was loaded on a DEAE-cellulose column (2.6 by 23 cm) equilibrated with buffer B. The column was washed with 400 ml of buffer B and eluted with a linear 0 to 800 mM KCl gradient in buffer B. Ten 6-ml fractions with high levels of GA3PDH activity were pooled and concentrated, and the buffer was changed to buffer C. This pooled, concentrated sample was loaded onto a hydroxyapatite column (2.5 by 10 cm) equilibrated with buffer C. The column was washed with 200 ml of buffer C and eluted with a linear 20 to 700 mM KPO_4 buffer (pH 7.2) in buffer C. Twelve 4-ml fractions with high levels of GA3PDH activity were pooled and concentrated, and the buffer was changed to buffer C. SDS–15% PAGE (5.6% stacking gel) (37) followed by staining with Coomassie brilliant blue R-250 showed that GA3PDH was purified to apparent homogeneity at this stage (data not shown). Glycerol was added to 15% (vol/vol), and purified GA3PDH samples were divided into 0.5-ml aliquots and stored at −75°C (above).

Biochemical characterization of purified E4PDH. The native molecular mass of the purified E4PDH was determined on a calibrated Sephadex G-200 column (2.6 by 70 cm) equilibrated with buffer A. The subunit molecular mass was determined by SDS-PAGE (Fig. 2). The sequence of the amino terminus of purified E4PDH was determined as described previously (59). The amino terminus of the polypeptide was Thr-Val-?-Val-Ala-Ile-Asn-Gly-Phe-Gly-Arg-Ile, which matched exactly the one predicted from the *gapB* DNA sequence (1), except that the amino-terminal methionine residue was removed and there was an ambiguity at position 4. The predicted amino acid at position 4 was an arginine residue. The sequence analysis indicated an amino acid at position 4 similar, but not identical, to proline (data not shown). Heat stability of E4PDH was determined by heating mixtures (0.2 ml) containing 20 mM KPO_4 buffer (pH 8.2), 1 mM DTT, and 24 μg of purified E4PDH for 5 min at temperatures ranging from 40 to 60°C, followed by rapid chilling. An aliquot (0.5 μg) of the heat-treated mixture was assayed for E4PDH activity at 37°C as described above. The temperature and pH optima of the E4PDH reaction were determined in mixtures (1 ml) containing 50 mM PP_i buffer, 1 mM DTT, 1.2 mM NAD^+, 1 mM E4P, 125 μg of BSA, and 1 μg of purified E4PDH. For the pH optimum, the pH was varied from 6 to 10 with phosphoric acid, and NADH formation was monitored by the increase in A_{340} at 37°C for 3 min. For the temperature optimum, the pH of the reaction mixture was 8.6, which was near the optimum, and NADH formation was determined for 3-min reactions at temperatures ranging from 20 to 60°C.

PdxB dehydrogenase assay. The *pdxB* and *serC*(*pdxF*) reading frames were fused to the polyhistidine-encoding leader provided by vector pET15b by standard cloning and PCR methods (43, 47). In each case, an *Nde*I restriction site was engineered by PCR to the amino-terminal end of the reading frames to allow

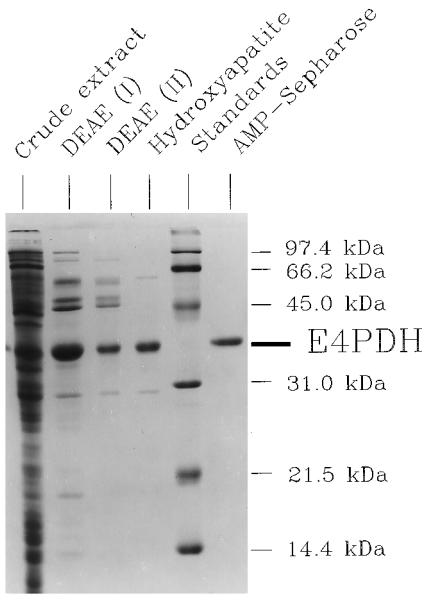

FIG. 2. SDS-PAGE analysis of samples from different stages of purification of *E. coli gapB* (*epd*)-encoded dehydrogenase from strain JM109(pTX420 *gapB*$^+$ [epd$^+$]). The purification scheme is summarized in Table 1 and described in Materials and Methods. SDS-PAGE on 15% (wt/vol) polyacrylamide gels (5.6% stacking) and Coomassie blue staining were performed as described in Materials and Methods. Lanes (from left) contained crude extract (50 μg), pooled fractions from the first DEAE-cellulose column (24 μg), pooled fractions from the second DEAE-cellulose column (5 μg), pooled hydroxyapatite column fractions (5 μg), polypeptide molecular mass standards (≈3 μg each), and pooled AMP-Sepharose column fractions (4 μg). Fractions were pooled on the basis of E4PDH activity.

in-frame fusion to the leader. The resulting plasmids pTX359 (His-6–PdxB) and pTX358 [His-6–SerC(PdxF)] were transformed in strain TX2687, which is a *pdxB serA recA1* lysogen of λDE3. Plasmid pTX359 (His-6–PdxB) complemented the *pdxB* mutation in TX2687 even in the absence of IPTG induction; thus, the His-6–PdxB protein was at least partially active in vivo. His-6–PdxB and His-6–SerC(PdxF) were overexpressed and purified to near homogeneity by batch chromatography at room temperature following the manufacturer's instructions, except that cells were lysed in a French pressure cell (as described above) instead of by sonication. Following elution from the charged $NiSO_4$ resin, the purified proteins were desalted and the buffer was changed to 20 mM KPO_4 buffer (pH 6.2)–1.0 mM DTT–1 mM EDTA–5% glycerol by using PD-10 columns (Pharmacia LKB Biotechnology). Glycerol was added to 30% (vol/vol), and the protein samples were divided into 1.0-ml aliquots stored at −75°C. The purified His-6–PdxB and His-6–SerC(PdxF) proteins gave single bands with predicted molecular masses in Coomassie-stained SDS-PAGE; breakdown products or contaminating proteins were minimal (data not shown). Purified His-6–SerC (PdxF) protein showed substantial transaminase activity when assayed as described previously (20).

His-6–PdxB dehydrogenase assays were modeled on those used to determine the forward reaction of the PdxB homolog, 3-phosphoglycerate dehydrogenase (3PGDH), encoded by *serA* (56). Reaction mixtures contained 64 mM Tris-HCl (pH 8.5), 41 mM ammonium acetate, 2.6 mM potassium glutamate, 0.8 mM DTT, 25 or 50 μg of His-6–PdxB, 25 or 50 μg of His-6–SerC(PdxF), 280 μM acetylpyridine adenine dinucleotide ($APAD^+$) or NAD^+, and the concentrations of putative substrates indicated in Table 3 (see Results). By analogy to the SerA reaction, which favors the reverse direction (44), we included the purified His-6–SerC(PdxF) enzyme and glutamate in reaction mixtures in an attempt to drive the His-6–PdxB reaction forward. APADH or NADH formation was monitored by the increase in fluorescence intensity (excitation at 340 nm, emission at 425 or 465 nm) with a Hitachi F-2000 fluorescence spectrophotometer equipped with a kinetics mode and stirred cell (56). All reaction mixture components except substrates were mixed at 25°C, and the background fluorescence was measured. Substrate was then added to the stirred cell, and the burst in fluorescence intensity due to NADH or APADH formation was measured. Control experiments showed that increases in fluorescence intensity depended on the presence of the substrates and were proportional to the amount of His-6–PdxB protein added.

A fraction of the His-6–PdxB protein contained tightly bound NADH, as indicated by a characteristic fluorescent peak centered at 425 nm (excitation, 340 nm; data not shown), which is shifted from the 465-nm fluorescence emission peak for free NADH. A similar 425-nm fluorescence peak was reported previously for NADH bound to purified SerA 3PGDH (56). Yet, most of the tightly bound cofactor which bound to His-6–PdxB was nonfluorescent NAD^+, because the added substrates, such as 4PE, were oxidized, with concomitant reduction of NAD^+ and an increase in bound NADH fluorescence (see Table 3). Because the tightly bound cofactor was not discovered until later experiments, most assays were performed at an emission wavelength (465 nm) that did not correspond to the maximum for bound NADH (425 nm) (see Results). Experiments repeated at 425 nm gave essentially the same results as those obtained at 465 nm (see Table 3), except the background fluorescence before substrate addition was about threefold higher at 425 nm than at 465 nm (data not shown). The addition of free NAD^+ to reaction mixtures did not lead to sustained oxidation of the substrate or catalytic formation of free NADH (emission peak centered at 465 nm). His-6–SerC(PdxF) slightly stimulated (≤twofold) the final fluorescence intensity reached in the reactions, but His-6–SerC(PdxF) did not lead to sustained coupled reactions (see Table 3; data not shown). Dialysis of His-6–PdxB protein failed to remove tightly bound NAD^+ and NADH or lead to a sustained reaction (see above; data not shown). Unlike native SerA 3PGDH, which is a homotetramer (56), purified His-6–PdxB protein was a homodimer (data not shown). Removal of the His-6–peptide from His-6–PdxB with thrombin was difficult compared with our experience with other proteins, and the resulting PdxB protein still did not sustain the dehydrogenase reaction (data not shown).

The products of the E4PDH reactions were treated with activated charcoal (53) to remove NAD^+ and NADH before being tested as possible substrates for the PdxB dehydrogenase reaction. E4PDH reaction mixtures were incubated twice with 10% (vol/vol) prewetted, activated charcoal at room temperature for 30 min. The charcoal was removed by brief centrifugation in a microcentrifuge. NAD^+ and NADH remaining in the supernatant were monitored by A_{260} and fluorescence emission at 465 nm (excitation 340 nm), respectively. Residual unreacted E4P was measured by the E4PDH enzyme assay (above) run to completion.

Parameters used in calculations. The following parameters were used to calculate the number of enzyme molecules per cell and cellular enzyme concentrations: amount of protein recovered per 10^9 cells in extracts prepared as described above from bacteria grown exponentially in minimal medium plus glucose at 37°C (330 μg of protein per 10^9 cells [59]), Avogadro's number (6.023×10^{23} molecules/mol), the molecular mass of *gapA*-encoded GA3PDH (144 kDa) (12), the molecular mass of *gapB*-encoded E4PDH (132 kDa) (see Results), the average volume of an *E. coli* cell in a culture growing exponentially at a doubling time of about 1 h (0.8×10^{-12} ml per cell) (16), and cellular concentration of E4PDH (940 molecules per cell, ≈2 μM). The other kinetic parameters used to estimate catalytic capacities from the Michaelis-Menten equation are described in Results.

RESULTS

Purification of the dehydrogenase encoded by *E. coli* K-12 *gapB*. We amplified the *gapB* gene from *E. coli* K-12 chromosomal DNA, using high-fidelity PCR (see Materials and Methods). The amplified *gapB* gene was cloned into vectors pBR322 and pUC19, and the resulting plasmids were transformed in strains DH5α and JM109, respectively (see Materials and Methods). We then assayed E4PDH activity in crude extracts of several strains grown to late exponential phase (90 Klett [660 nm] units) in LB plus 50 μg of ampicillin per ml at 37°C. We obtained the following E4PDH-specific activities: 14.6 U/mg, DH5α(pBR322); 14.1 U/mg, JM109(pUC19); 133 U/mg, DH5α(pTX419 *gapB*$^+$); 486 U/mg, JM109(pTX420 *gapB*$^+$) grown without IPTG; and 649 U/mg, JM109(pTX420 *gapB*$^+$) grown with IPTG. Thus, E4PDH-specific activity was increased 9- to 46-fold by multicopy vectors. Most of this increase in E4PDH activity was apparently due to expression from an endogenous *gapB* promoter (1) and vector copy number, because the addition of IPTG stimulated E4PDH synthesis only about 1.3-fold for plasmid pTX420, which had *gapB* fused to the P_{lac} promoter of pUC19 (see Materials and Methods). These findings were the first indication that *gapB* encoded E4PDH.

We purified the *gapB*-encoded E4PDH from strain JM109 (pTX420 *gapB*$^+$) to electrophoretic homogeneity by the scheme shown in Table 1 and illustrated in Fig. 2. We confirmed that the amino acid sequence predicted from the DNA sequence of *gapB*$^+$ in pTX420 exactly matched that reported previously (see Materials and Methods) (1). Several features of

TABLE 1. Purification of *gapB* (*epd*)-encoded dehydrogenase from *E. coli* K-12 strain JM109(pTX420)[a]

Fraction	Total protein (mg)	Sp act (U/mg)	Total activity (U)	Purification (fold)	Yield (%)
Crude extract	1,440	239	369,000	≡1	≡100
DEAE-cellulose					
(I)	110	4,790	527,000	20	143
(II)	56	9,470	530,000	40	144
Hydroxyapatite	23	17,100	393,000	72	107
5′-AMP Sepharose-affinity resin	9.4	21,400	199,000	88	54

[a] For details about enzyme overexpression, enzyme assays, and this purification scheme, see Materials and Methods.

TABLE 2. Substrate specificity of dehydrogenases encoded by *gapB* and *gapA*

Substrate[a]	Dehydrogenase activity[b]	
	gapB (*epd*) encoded[c]	*gapA* encoded (GA3PDH)
2 mM E4P + 2 mM NAD^+	75.3	25.0
2 mM E4P + 2 mM NAD^+ + 30 mM arsenate	68.5	29.4
2 mM E4P + 2 mM $APAD^+$	10.0	10.1
2 mM E4P + 2 mM $NADP^+$	2.3	1.9
0.1 mM GA3P + 2 mM NAD^+[d]	0.47	29.0
0.1 mM GA3P + 2 mM NAD^+ + 30 mM arsenate[d]	0.84	36.5
2 mM GA3P + 2 mM NAD^+	1.6	112.1
2 mM GA3P + 2 mM NAD^+ + 30 mM arsenate	1.6	137.1

[a] Reaction mixtures are described in Materials and Methods.
[b] Activities are expressed in nanomoles of NADH or APADH synthesized by 0.5 μg of purified enzyme in a 0.5-ml reaction mixture at 37°C in 3 min. *gapB* (*epd*)-encoded dehydrogenase reactions were linear for 3 min in all cases, whereas GA3PDH reactions lacking arsenate became nonlinear within this time interval because of product inhibition (12, 26).
[c] Negligible *gapB* (*epd*)-encoded dehydrogenase activity was detected in reaction mixtures containing 2 mM (each) G6P, D-ribose-5-phosphate, D-arabinose-5-phosphate, or D-erythrose (data not shown).
[d] Represents the approximate GA3P contamination concentration in a 2 mM E4P solution.

this purification scheme are noteworthy. There was a large increase in E4PDH specific activity after the first two DEAE-cellulose column steps (Table 1). This increase in specific activity suggested that an inhibitor was removed. A similar increase in specific activity was observed during the purification of *gapA*-encoded GA3PDH (12). *gapB*-encoded E4PDH bound more tightly to DEAE-cellulose at pHs of 7.5 and 8.2 than *gapA*-encoded GA3PDH. This property was consistent with the predicted pI values of E4PDH (6.75) (1) and GA3PDH (7.11) (8) and allowed partial separation of the two enzymes. The key to the purification scheme was the observation that E4PDH failed to bind to hydroxyapatite, whereas GA3PDH bound strongly in 20 mM KPO_4 buffer at pH 7.2 (see Materials and Methods). Chromatography of the last 5′-AMP–Sepharose-affinity column was necessary to remove two persistent, residual, contaminating polypeptides (Fig. 2, lane 4). We established that purified E4PDH was encoded by the cloned *gapB* gene by sequencing the amino terminus of the purified protein (see Materials and Methods). The molecular mass of purified E4PDH (35 kDa; Fig. 2, lane 6) matched the 37,298-Da molecular mass predicted from the *gapB* DNA sequence (1).

Biochemical properties of *gapB*-encoded E4PDH. We investigated the substrate specificity of the purified E4PDH protein to determine if it was specific for E4P or whether it could also use GA3P as a substrate (Table 2). For comparison, we devised a streamlined, two-step protocol for the purification of *gapA*-encoded GA3PDH to apparent homogeneity (see Materials and Methods). GA3PDH catalyzes the reversible oxidative phosphorylation of GA3P to form 1,3-diphosphoglycerate (12, 22, 26, 45). In the presence of arsenate instead of P_i, the GA3PDH reaction becomes irreversible and forms 1-arseno-3-phosphoglycerate, which spontaneously decomposes to 3-phosphoglycerate (12, 26). The *gapB*-encoded dehydrogenase was specific for E4P as a substrate and NAD^+ as a cofactor, and this reaction was not stimulated by 30 mM arsenate (Table 2, column 2). GA3P and G6P, which were contaminants in E4P (see Materials and Methods and below), and $NADP^+$ were not used by the *gapB*-encoded enzyme under these assay conditions. $APAD^+$, an NAD^+ analog, was used by the *gapB*-encoded E4PDH much less efficiently than NAD^+ (Table 2, line 3). As expected, *gapA*-encoded GA3PDH efficiently used GA3P as a substrate, and the GA3PDH activity was stimulated by 30 mM arsenate (Table 2, lines 7 and 8) (12, 26, 45). GA3PDH showed an apparent activity with E4P as a substrate (Table 2, lines 1 and 2); however, this activity was due entirely to the 0.1 mM GA3P contamination in the 2 mM E4P preparation (Table 2, lines 5 and 6). Thus, *gapA*-encoded GA3PDH was specific for GA3P and exhibited minimal activity with E4P under these assay conditions. In contrast, *gapB*-encoded E4PDH was specific for E4P and did not use GA3P as a substrate. Moreover, E4PDH probably does not carry out both oxidation and phosphorylation as does GA3PDH, because the E4PDH reaction was not stimulated by arsenate (Table 2).

The results from experiments in which the E4PDH reaction proceeded to completion also supported the contention that *gapB* encodes E4PDH. The analysis provided by the manufacturer stated that the E4P preparation was only 67% pure (see Materials and Methods). Using this correction factor, we observed that reaction mixtures containing 0.2, 0.4, and 2 mM starting concentrations of E4P produced 0.17, 0.37, and 1.9 mM NADH, respectively, after 40 to 60 min at 37°C. Thus, nearly all of the E4P present could be oxidized in the E4PDH reaction. The identity of the product of the E4PDH reaction is considered below.

We characterized the biochemical and kinetic properties of *gapB*-encoded E4PDH further (see Materials and Methods). The purified protein had a native molecular mass of 132 kDa and thus appeared to be a tetramer of identical 37.2-kDa subunits (Fig. 2) (1). Purified E4PDH was stable for weeks at 4°C, with negligible loss of activity. E4PDH was relatively thermally stable and did not begin to lose significant activity until it was incubated at 50°C for 5 min (see Materials and Methods; data not shown). The temperature profile of E4PDH activity was bell shaped, with a maximum of 50°C at pH 8.6, which was near the pH optimum (see Materials and Methods; data not shown). The pH profile rose steeply between pH 7 and 9 and then dropped slightly at pH 10 (data not shown). Purified E4PDH required the presence of a reducing agent, such as DTT or β-mercaptoethanol, to maintain activity. When E4PDH was dialyzed overnight at 4°C against 10 mM KPO_4 buffer (pH 7.5) without a reducing agent, E4PDH specific activity dropped about 10-fold. Incubation of dialyzed E4PDH in the same buffer containing 1 mM DTT or 3 mM β-mercaptoethanol for 3 h at 4°C restored the E4PDH specific activity to 45 or 27%, respectively, of that of the starting undialyzed

enzyme (data not shown). The kinetic parameters of the E4PDH reaction were determined by standard steady-state methods in which one substrate was fixed at a saturating level while the amount of the other was varied (see Materials and Methods) (data not shown) (49a). The apparent K_m value for substrate E4P [K_m^{app}(E4P)] was 0.96 ± 0.13 mM, where E4P concentrations were corrected as described above. The K_m^{app} (NAD^+) value was 0.074 ± 0.011 mM. The apparent V_{max} value for substrate E4P [V_{max}^{app}(E4P)] and V_{max}^{app}(NAD^+) values were approximately equal at $91.2 \times 10^3 \pm 5.9 \times 10^3$ U/mg (apparent k_{cat} catalytic constant [k_{cat}^{app}] = 200 s^{-1}) and $77.2 \times 10^3 \pm 2.0 \times 10^3$ U/mg (k_{cat}^{app} = 169 s^{-1}), respectively, where for the k_{cat}^{app} calculations it was assumed that all purified E4PDH was active.

Cellular concentration of E4PDH. We used the specific activity of purified E4PDH to calculate a lower limit of the cellular concentration of E4PDH. The specific activity of purified E4PDH was 21,400 U/mg (Table 1), and the specific activity of E4PDH was 13.4 U/mg in crude extracts of bacteria grown exponentially with shaking in minimal salts medium plus glucose at 37°C (see Materials and Methods). From these values and other parameters presented in Materials and Methods, we calculated that there are at least 940 E4PDH tetramers per bacterial cell growing under these conditions. This minimal estimate assumes that all of the purified E4PDH enzyme was active and that no inhibition of E4PDH activity occurred in the crude extracts, which is probably not the case. Thus, E4PDH is a moderately abundant cellular enzyme (see Discussion) (59).

Analysis of the product of E4PDH reaction. We analyzed the substrate preparation and products of the E4PDH reaction mixture containing E4P and NAD^+ by TLC on microcrystalline cellulose plates (see Materials and Methods). The commercially available E4P preparation gave two smeared purple spots of about equal intensities (R_f of ≈0.33 and 0.18) in response to the Hanes-Isherwood reagent for phosphate-sugar compounds (see Materials and Methods) (data not shown). Bromine oxidation of the E4P preparation converted the two spots into one distinct 4PE spot with an intermediate of mobility (R_f of ≈0.25). Since both major spots in the E4P preparation were converted into 4PE, the two spots likely represented the chromatographically distinct monomer and covalent dimer species of E4P observed previously (5, 55). E4PDH reaction mixtures whose reactions were taken to completion were spotted onto the same TLC plates. The E4PDH reaction converted the majority of the two E4P spots to one species with an R_f of ≈0.24, which matched the R_f value of 4PE synthesized by bromine oxidation of E4P. Thus, the product of E4PDH reactions containing E4P and NAD^+ was likely 4PE. The 24% contamination other than that by GA3P (≈6% [mol/mol]) and G6P (≈3% [mol/mol]) in the E4P preparations was probably not a phosphate sugar, because it was not detectable with the Hanes-Isherwood reagent.

We also investigated whether the product of the E4PDH reaction could serve as a substrate for the PdxB dehydrogenase (Fig. 1). PdxB dehydrogenase activity has been difficult to detect in extracts from overexpressing strains, and lack of a reliable assay has impeded purification of the native enzyme (43a, 60). Therefore, we purified the PdxB dehydrogenase and the SerC(PdxF) transaminase by histidine-tag-affinity chromatography (43) and set up the assay system described in Materials and Methods. Oxidation of putative substrates was monitored by reduction of NAD^+ to NADH, which remained tightly bound to the PdxB dehydrogenase (see Materials and Methods) (Table 3). 4PE and to a lesser extent 3PG, which is the substrate of the *serA*-encoded 3PGDH (44, 56), caused significant reduction of bound NAD^+ (11.4- and 5.4-fold, respectively) (Table 3). Other phosphate-sugar compounds and contaminants in the chemically synthesized 4PE were not likely substrates of the PdxB enzyme (Table 3, 1.4- to 2.6-fold). Neither 0.8 mM 4PE nor 0.8 mM 3PG led to sustained reactions with catalytic conversion of added NAD^+ to free NADH (see Materials and Methods). Possible reasons for this lack of a sustained reaction, such as strong product inhibition, lack of a protein subunit, suboptimal reaction conditions, and aberrant properties of the His-6–tag-purified enzymes, are being investigated. Nonetheless, the specificity of these data strongly suggests that 4PE, and possibly D-3-phosphoglycerate (3PG), are substrates of the PdxB dehydrogenase.

We tested whether the products of E4PDH reactions also stimulated reduction of the NAD^+ cofactor bound tightly to the His-6–PdxB dehydrogenase (Table 3). To perform these assays, we first treated the products of E4PDH reactions with activated charcoal to remove NAD^+ and NADH (see Materials and Methods). The product of E4PDH reactions containing E4P and NAD^+ as substrates stimulated the reduction of bound NAD^+ to NADH by the His-6–PdxB dehydrogenase (8.4-fold) (Table 3). Phosphate-sugar contaminants in the

TABLE 3. Putative substrates of PdxB dehydrogenase reaction[a]

Substrate (type of mixture)	Increase (fold) in NADH fluorescence in PdxB reaction
Chemical	
0.8 mM 4PE[b]	11.4
0.08 mM E4P (control)[b]	1.5
0.06 mM 3PG (control)[b]	2.4
0.03 mM D-6-phosphogluconate (6PG) (control)[b]	1.4
0.8 mM 3PG	5.4
0.8 mM E4P	2.6
0.8 mM 6PG	2.1
2.0 mM D-erythronate	1.4
Enzymatic[c]	
E4PDH and 4 mM E4P (reaction)	8.4
BSA and 4 mM E4P (control)	1.8
E4PDH and 0.29 mM GA3P (control)	1.0
BSA and 0.29 mM GA3P (control)	1.0
E4PDH and 0.15 mM G6P (control)	1.0
BSA and 0.15 mM G6P (control)	1.0

[a] PdxB dehydrogenase reaction mixtures contained both the His-6–PdxB and His-6–SerC(PdxF) proteins (see Materials and Methods). NADH formation is expressed as the fold increase in fluorescence intensity above background (excitation at 340 nm; emission at 465) after substrate addition. The starting fluorescence before substrate addition was about 73 or 95 (arbitrary) U for reaction mixtures containing chemical substrates or treated reaction products, respectively. The PdxB dehydrogenase reaction was not sustained with time (see Results); hence, steady-state kinetic parameters are not given. Other properties of the PdxB dehydrogenase reaction are described in Materials and Methods.

[b] 4PE was synthesized by bromine oxidation of E4P (see Materials and Methods). Chemically synthesized 4PE was contaminated with unreacted E4P (≈10%) and 3PG (≈8%) and 6PG (≈4%), which were formed from GA3P and G6P contaminants in E4P. Contaminant levels were determined enzymatically (see Materials and Methods). The control reaction mixtures contained samples of pure compounds at the concentrations at which they contaminated the 0.8 mM 4PE preparation.

[c] Reaction mixtures containing the indicated substrates and proteins were monitored to completion (see Materials and Methods). The NADH formed was removed by absorption to activated charcoal, and treated supernatants were used as substrates for the PdxB dehydrogenase reaction (see Materials and Methods). The amount of treated product mixture added to PdxB reaction mixtures would give a final 4PE concentration of 0.8 mM if all initial E4P were converted to 4PE and no 4PE were lost during the charcoal extractions. Contaminant levels in treated product reaction mixtures containing E4PDH and E4P were measured enzymatically (7% [mol/mol] GA3P; 4% [mol/mol] G6P) (see Materials and Methods) and used to design the control experiments shown. The product of reaction mixtures containing E4PDH and E4P was also monitored by TLC (see Results).

product mixtures, such as GA3P and G6P, were not responsible for the increased formation of bound NADH (Table 3, controls). These results confirmed the conclusion that 4PE was the likely product of the oxidation of E4P by the GapB E4PDH and that 4PE is a likely substrate of the PdxB dehydrogenase.

DISCUSSION

Four lines of evidence strongly implicate 4-carbon phosphate-sugar compounds as direct intermediates of carbons 5′, 5, and 6 of the pyridine ring of PLP (Fig. 1). First, PLP biosynthesis is dependent on the transketolase function that produces the important common intermediate E4P (58). Second, 4HT supplements *pdxB* mutants unable to synthesize PLP (19). Third, the PdxB enzyme is a member of a family of D-isomer-specific 2-hydroxy-acid dehydrogenases that includes the *serA*-encoded 3PGDH, which uses a 3-carbon phosphate-sugar compound as its substrate (39, 43, 48). Fourth, the SerC(PdxF) transaminase is required for both the major phosphorylated L-serine and PLP biosynthetic pathways (15, 39). The model for PLP biosynthesis from 4-carbon phosphate-sugar compounds (Fig. 1) requires the activity of an E4PDH, but such an enzyme has never been purified (39). In this report, we show that the *E. coli* K-12 *gapB* gene encodes a tetrameric E4PDH, rather than a second GA3PDH. In addition, we demonstrate that the product of the E4PDH reaction, 4PE, is likely a substrate of PdxB dehydrogenase (Tables 2 and 3) (see Results). Thus, the *gapB*-encoded E4PDH may play a role in de novo PLP biosynthesis.

Three reasons could account for the fact that *gapB* was not identified previously in extensive hunts for mutants that require PN for growth (14, 15, 38). First, *gapB* is immediately upstream of the *pgk* glycolytic gene (see Introduction) (1, 22, 33, 34). If *gapB* is contranscribed with *pgk* in vivo, *gapB* mutations may exert polarity on *pgk* expression. Yet, all previous *pdx* mutant hunts were done with minimal medium containing only glucose or glycerol as a carbon source. Neither medium supports the growth of *pgk* mutants, which require minimal medium supplemented with glycerol and succinate or malate (22, 33, 34). Second, *gapA*-encoded GA3PDH may provide enough residual E4PDH activity in cells starving for PN to allow slow growth of *gapB* mutants. *E. coli gapA*-encoded GA3PDH did not use E4P as a substrate under in vitro assay conditions used in this study (Table 2). But, GA3PDH is highly abundant and represents about 5% (wt/wt) *E. coli* cellular protein (12, 26, 60), which amounts to about 71,000 GA3PDH tetramers per bacterial cell (see Materials and Methods). By contrast, there are only about 940 *gapB*-encoded E4PDH tetramers per cell (see Results). Low levels of E4PDH activity were detected from purified mammalian GA3PDH by using the same assay conditions described above (see Introduction) (36, 45); however, the possibility that this low level of E4PDH activity was due to a small amount of a contaminating enzyme cannot be completely ruled out. Third, 4PE might be required for the synthesis of another compound besides PLP; therefore, *gapB* mutants would not be detected in screens for PN auxotrophy. This possibility seems unlikely, because *tktA tktB* double mutants, which cannot synthesize E4P, required only PN and the three aromatic amino acids and vitamins for growth (58). Genetic experiments in progress will test the hypothesis that *gapB*-encoded E4PDH plays a direct role in PLP biosynthesis.

The three isoenzymes of 3-deoxy-D-*arabino*-heptulosonate 7-phosphate (DAHP) synthase are the only other enzymes known to use E4P as a substrate in *E. coli*, besides the E4PDH reported here (10, 42, 49, 52). The DAHP synthase isoenzymes catalyze the first step in the common pathway leading to the biosynthesis of the aromatic amino acids and vitamins (Fig. 1) (10, 42, 49, 52). To our knowledge, the intracellular concentration of E4P has not been reported for *E. coli* (3, 18, 28), and E4P has been difficult to detect as a free intermediate in plant and animal tissues (18, 55). The K_m values of the DAHP synthases range from 50 to 100 μM (10, 42, 49, 52), which may give an indication of the intracellular *E. coli* E4P concentration (49a). In comparison, the apparent affinity of E4PDH for E4P is at least an order of magnitude lower [K_m^{app}(E4P) = 1,000 μM] (see Results). This relatively low substrate affinity is consistent with E4PDH playing a role in PLP coenzyme biosynthesis, because the PLP biosynthetic proteins are relatively abundant but kinetically limited enzymes (14, 54, 59). E4PDH fits this pattern; it is present in about 940 tetramers per cell (see Results), has a high apparent affinity for NAD^+ (K_m^{app} (NAD^+) = 75 μM, compared with the total intracellular NAD^+ concentration of 790 μM [6]), turns E4P over rapidly (k_{cat}^{app}(E4P) = 200 s^{-1}), but binds E4P poorly compared with the DAHP synthases. Nevertheless, if the intracellular E4P concentration is about 50 μM in bacteria growing in minimal salts medium plus glucose with a doubling time of 1 h, there would be enough E4PDH catalytic capacity to synthesize about 3.5×10^6 molecules of 4PE per cell per h (see Materials and Methods), which is still approximately 50 times greater than the capacity needed to meet the low net rate of B_6-vitamer biosynthesis ($\approx 6.5 \times 10^4$ molecules of B_6-vitamers per cell per h) (14, 59). A 50-fold excess of catalytic capacity was also calculated for PNP/PMP oxidase (59). For these calculations, it was assumed that the kinetic properties determined in vitro apply in vivo and that does not occur in vivo inhibition of enzyme activity (see above) (59).

We tested several nucleotides with structures related to NAD^+ (cAMP, AMP, ADP, and ATP) and PLP biosynthetic intermediates (PNP, PN, 4HT, pyridoxal, and PLP [Fig. 1]) for inhibition of E4PDH activity (see Materials and Methods). With the exception of PLP, none of these other compounds affected the E4PDH reaction. We were unable to test 4PHT, which may be the product of this branch of the PLP biosynthetic pathway (Fig. 1) (see Introduction), because 4PHT is not available. PLP inhibition of E4PDH activity was competitive with the substrate E4P (K_i^{app} = 100 μM). However, this PLP inhibition is probably not of physiological significance, because the total intracellular concentration of all B_6-vitamers is only about 100 μM (59). In comparison, PNP/PMP oxidase is competitively inhibited by PLP with a K_i of only 8 μM (59).

Our finding that *gapB* actually encodes an E4PDH lacking detectable GA3PDH activity has important implications for the analyses of GA3PDH evolution. The presence of two possible *gap* genes in *E. coli* has not been understood (17, 41, 42a). *E. coli gapA* (*gap1*) is closely related to *gap* genes that encode cytosolic GA3PDH in eukaryotes (41). *E. coli gapB* (*gap2*) is most related to eubacterial *gap* genes found adjacent to *pgk* and to the cyanobacterial *gap3* gene (17, 41). Some of these *gapB*-related genes are known to encode active GA3PDH (11, 21), unlike *E. coli gapB* itself (see Results) (1). Our findings support the interpretation that *E. coli gapA* and *gapB* arose by duplication of an ancestral eubacterial gene (41, 42a). The different function of *E. coli gapB* may explain why it does not fit easily into bacterial phylogeny schemes based on *gap* genes (17, 41, 42a). One interpretation consistent with bacterial *gap* gene evolutionary relationships is that the ancestral enzyme had both GA3PDH and E4PDH activities. Following duplication, the *E. coli gapA* gene evolved to encode a GA3PDH largely lacking E4PDH activity. Meanwhile, *E. coli gapB*, which was still linked to *pgk*, specialized to encode an E4PDH required for PLP biosynthesis. If this scenario is correct, then the

GA3PDH encoded by *gap* genes closely related to *E. coli gapB*, such as those from *Zymomonas mobilis* and *Corynebacterium glutamicum* (11, 21, 41), may still retain E4PDH activity. Since *E. coli gapB* encodes an E4PDH that lacks detectable GA3PDH activity, even at high enzyme and substrate concentrations, we propose renaming *gapB* as *epd* (for D-erythrose-4-phosphate dehydrogenase).

ACKNOWLEDGMENTS

We thank I. D. Spenser for a sample of 4-hydroxy-L-threonine, I. D. Spenser and R. E. Hill for a preprint of their review on pyridoxine biosynthesis, and K. Herrmann and R. Bauerle for information about E4P concentrations in *E. coli*. We thank B. Bachmann, C. Yanofsky, and G. Weinstock for bacterial strains used in this study and T.-K. Man and C. Liang for helpful discussions and advice.

This work was supported by Public Health Service grant RO1-37561 from the National Institute of General Medical Sciences.

REFERENCES

1. **Alefounder, P. R., and R. N. Perham.** 1989. Identification, molecular cloning, and sequence analysis of a gene cluster encoding the class II fructose 1,6-biphosphate aldolase, 3-phosphoglycerate kinase, and a putative second glyceraldehyde 3-phosphate dehydrogenase of *Escherichia coli*. Mol. Microbiol. **3:**723–732.
2. **Arps, P. J., C. C. Marvel, B. C. Rubin, D. A. Tolan, E. E. Penhoet, and M. E. Winkler.** 1985. Structural features of the *hisT* operon of *Escherichia coli* K-12. Nucleic Acids Res. **13:**5297–5315.
3. **Bauerle, R.** 1995. Personal communication.
4. **Bender, D. A.** 1985. Amino acid metabolism. John Wiley & Sons, New York.
5. **Blackmore, P. F., J. F. Williams, and J. K. MacLeod.** 1976. Dimerization of erythrose 4-phosphate. FEBS Lett. **64:**222–226.
6. **Bochner, B. R., and B. N. Ames.** 1982. Complete analysis of cellular nucleotides by two-dimensional thin layer chromatography. J. Biol. Chem. **257:** 9759–9769.
7. **Bradford, M. M.** 1976. A rapid and sensitive method for the quantitation of microgram quantities of protein utilizing the principle of protein-dye binding. Anal. Biochem. **72:**248–254.
8. **Branlant, G., and C. Branlant.** 1985. Nucleotide sequence of the *Escherichia coli gap* gene. Eur. J. Biochem. **150:**61–66.
9. **Branlant, G., G. Flesch, and C. Branlant.** 1983. Molecular cloning of the glyceraldehyde 3-phosphate dehydrogenase genes of *Bacillus stearothermophilus* and *Escherichia coli*, and their expression in *Escherichia coli*. Gene **25:**1–7.
10. **Camakaris, J., and J. Pittard.** 1974. Purification and properties of 3-deoxy-D-arabinoheptulosonic acid-7-phosphate synthetase (trp) from *Escherichia coli*. J. Bacteriol. **120:**590–597.
11. **Conway, T., G. W. Sewell, and L. O. Ingram.** 1987. Glyceraldehyde 3-phosphate dehydrogenase gene from *Zymomonas mobilis*: cloning, sequencing, and identification of promoter region. J. Bacteriol. **169:**5653–5662.
12. **D'Alessio, G., and J. Josse.** 1971. Glyceraldehyde phosphate dehydrogenase, phosphoglycerate kinase, and phospholyceromutase of *Escherichia coli*: simultaneous purification and physical properties. J. Biol. Chem. **246:**4319–4325.
13. **Davis, R. W., D. Botstein, and J. R. Roth.** 1980. Advanced bacterial genetics. Cold Spring Harbor Laboratory, Cold Spring Harbor, N.Y.
14. **Dempsey, W. B.** 1980. Biosynthesis and control of vitamin B_6 in *Escherichia coli*, p. 93–111. *In* G. P. Tryfiates (ed.), Vitamin B_6 metabolism and role in growth. Food and Nutrition Press, Westport, Conn.
15. **Dempsey, W. B.** 1987. Synthesis of pyridoxal phosphate, p. 539–543. *In* F. C. Neidhardt, J. L. Ingraham, K. B. Low, B. Magasanik, M. Schaechter, and H. E. Umbarger (ed.), *Escherichia coli* and *Salmonella typhimurium*: cellular and molecular biology. American Society for Microbiology, Washington, D.C.
16. **Donachie, W. D., and A. C. Robinson.** 1987. Cell division: parameter values and the process, p. 1578–1593. *In* F. C. Neidhardt, J. L. Ingraham, K. B. Low, B. Magasanik, M. Schaechter, and H. E. Umbarger (ed.), *Escherichia coli* and *Salmonella typhimurium*: cellular and molecular biology. American Society for Microbiology, Washington, D.C.
17. **Doolittle, R. F., D. F. Feng, K. L. Anderson, and M. R. Alberro.** 1990. A naturally occurring horizontal gene transfer from a eukaryote to a prokaryote. J. Mol. Evol. **31:**383–388.
18. **Draths, K. M., D. L. Pompliano, D. L. Conley, J. W. Frost, A. Berry, G. L. Disbrow, R. J. Staversky, and J. C. Lievence.** 1992. Biocatalytic synthesis of aromatics from D-glucose: the role of transketolase. J. Am. Chem. Soc. **114:**3956–3962.
19. **Drewke, C., C. Notheis, U. Hansen, E. Leistner, T. Hemscheidt, R. E. Hill, and I. D. Spenser.** 1993. Growth response to 4-hydroxy-L-threonine of *Escherichia coli* mutants blocked in vitamin B_6 biosynthesis. FEBS Lett. **318:**125–128.
20. **Duncan, K., and J. R. Coggins.** 1986. The *serC-aroA* operon of *Escherichia coli*: a mixed function operon encoding enzymes from two different amino acid biosynthetic pathways. Biochem. J. **234:**49–57.
21. **Eikmanns, B. J.** 1992. Identification, sequence analysis, and expression of a *Corynebacterium glutamicum* gene cluster encoding the three glycolytic enzymes glyceraldehyde-3-phosphate dehydrogenase, 3-phosphoglycerate kinase, and triosephosphate isomerase. J. Bacteriol. **174:**6076–6086.
22. **Fraenkel, D. G.** 1987. Glycolysis, pentose phosphate pathway, and Entner-Doudoroff pathway, p. 142–150. *In* F. C. Neidhardt, J. L. Ingraham, K. B. Low, B. Magasanik, M. Schaechter, and H. E. Umbarger (ed.), *Escherichia coli* and *Salmonella typhimurium*: cellular and molecular biology. American Society for Microbiology, Washington, D.C.
23. **Fraenkel, D. G., and S. R. Levisohn.** 1967. Glucose and gluconate metabolism in an *Escherichia coli* mutant lacking phosphoglucose isomerase. J. Bacteriol. **93:**1571–1578.
24. **Hanahan, D., J. Jessee, and F. R. Bloom.** 1991. Plasmid transformation of *Escherichia coli* and other bacteria. Methods Enzymol. **204:**63–113.
25. **Hanes, C. S., and F. A. Isherwood.** 1949. Separation of the phosphoric esters on the filter paper chromatogram. Nature (London) **164:**1107–1112.
26. **Harris, J. I., and M. Waters.** 1976. Glyceraldehyde 3-phosphate dehydrogenase, p. 1–49. *In* P. D. Boyer (ed.), The enzymes, vol. 13. Academic Press, New York.
27. **Heath, J. D., J. D. Perkins, B. Sharma, and G. M. Weinstock.** 1992. *Not*I genomic cleavage map of *Escherichia coli* K-12 strain MG1655. J. Bacteriol. **174:**558–657.
28. **Herrmann, K. M.** 1995. Personal communication.
29. **Hill, R. E., B. G. Sayer, and I. D. Spenser.** 1989. Biosynthesis of vitamin B6: incorporation of D-1-deoxyxylulose. J. Am. Chem. Soc. **111:**1916–1917.
30. **Hillman, J. D., and D. G. Fraenkel.** 1975. Glyceraldehyde 3-phosphate dehydrogenase mutants of *Escherichia coli*. J. Bacteriol. **122:**1175–1179.
31. **Horecker, B. L.** 1957. Preparation and analysis of 6-phosphogluconate. Methods Enzymol. **3:**172–174.
32. **Hughes, K. T., and J. R. Roth.** 1984. Conditionally transposition-defective derivative of Mu d1 (Amp Lac). J. Bacteriol. **159:**130–137.
33. **Irani, M., and P. K. Maitra.** 1974. Isolation and characterization of Escherichia coli mutants defective in enzymes of glycolysis. Biochem. Biophys. Res. Commun. **56:**127–133.
34. **Irani, M. H., and P. K. Maitra.** 1976. Glyceraldehyde-3-P dehydrogenase, glycerate-3-P kinase and enolase mutants of *Escherichia coli*: genetic studies. Mol. Gen. Genet. **145:**65–71.
35. **Ishii, Y., T. Hashimoto, M. Tatibana, and H. Yoshikawa.** 1963. Erythronic acid 4-phosphate: an intermediate of inosine metabolism in human red cell hemolysates. Biochem. Biophys. Res. Commun. **10:**19–22.
36. **Kornberg, H. L., and E. Racker.** 1955. Enzymic reactions of erythrose 4-phosphate. Biochem. J. **61:**3–4.
37. **Laemmli, U. K.** 1970. Cleavage of structural proteins during the assembly of the head of bacteriophage T4. Nature (London) **227:**680–685.
38. **Lam, H.-M., E. Tancula, W. B. Dempsey, and M. E. Winkler.** 1992. Suppression insertions in the complex *pdxJ* operon of *Escherichia coli* K-12 by *lon* and other mutations. J. Bacteriol. **174:**1554–1567.
39. **Lam, H.-M., and M. E. Winkler.** 1990. Metabolic relationships between pyridoxine (vitamin B_6) and serine biosynthesis in *Escherichia coli* K-12. J. Bacteriol. **172:**6518–6528.
40. **Lam, H.-M., and M. E. Winkler.** 1992. Characterization of the complex *pdxH-tyrS* operon of *Escherichia coli* K-12 and pleiotrophic phenotypes caused by *pdxH* insertion mutations. J. Bacteriol. **174:**6033–6045.
41. **Martin, W., H. Brinkmann, C. Savonna, and R. Cerff.** 1993. Evidence for a chimeric nature of nuclear genomes: eubacterial origin of eukaryotic glyceraldehyde 3-phosphate dehydrogenase genes. Proc. Natl. Acad. Sci. USA **90:**8692–8696.
42. **McCandliss, R. J., M. D. Poling, and K. M. Herrmann.** 1978. 3-Deoxy-D-*arabino*-heptulosonate 7-phosphate synthase. J. Biol. Chem. **253:**4259–4265.

42a. **Nelson, K., T. S. Whittam, and R. K. Selander.** 1991. Nucleotide polymorphism and evolution in the glyceraldehyde-3-phosphate dehydrogenase gene (*gapA*) in natural populations of *Salmonella* and *Escherichia coli*. Proc. Natl. Acad. Sci. USA **88:**6667–6671.

43. **Pease, A. J., and M. E. Winkler.** 1993. Functional and evolutionary relationships between the *pdxB* and *serA* gene products of *Escherichia coli* K-12, abstr. K-116, p. 280. *In* Abstracts of the 93rd General Meeting of the American Society for Microbiology 1993. American Society for Microbiology, Washington, D.C.

43a. **Pease, A. J., and M. E. Winkler.** 1995. Unpublished results.

44. **Pizer, L. I.** 1963. The pathway and control of serine biosynthesis in *Escherichia coli*. J. Biol. Chem. **238:**3934–3944.
45. **Racker, E., V. Klybas, and M. Schramm.** 1959. Tetrose diphosphate, a specific inhibitor of glyceraldehyde 3-phosphate dehydrogenase. J. Biol. Chem. **234:**2510–2516.
46. **Roa, B. B., D. M. Connolly, and M. E. Winkler.** 1989. Overlap between *pdxA* and *ksgA* in the complex *pdxA-ksgA-apaG-apaH* operon of *Escherichia coli* K-12. J. Bacteriol. **171:**4767–4777.

47. **Sambrook, J., E. F. Fritsch, and T. Maniatis.** 1989. Molecular cloning: a laboratory manual, 2nd ed. Cold Spring Harbor Laboratory, Cold Spring Harbor, N.Y.
48. **Schoenlein, P. V., B. B. Roa, and M. E. Winkler.** 1989. Divergent transcription of *pdxB* and homology between the *pdxB* and *serA* gene products in *Escherichia coli*. J. Bacteriol. **171:**6084–6092.
49. **Schoner, R., and K. M. Herrmann.** 1976. 3-Deoxy-D-*arabino*-heptulosonate 7-phosphate synthase. J. Biol. Chem. **251:**5440–5447.
49a. **Segal, I. H.** 1975. Enzyme kinetics. John Wiley & Sons, New York.
50. **Silhavy, T. J., M. L. Berman, and L. W. Enquist.** 1984. Experiments with gene fusions. Cold Spring Harbor Laboratory, Cold Spring Harbor, N.Y.
51. **Simpson, F. J., A. S. Perlin, and A. S. Sieben.** 1966. Erythrose 4-phosphate. Methods Enzymol. **9:**35–38.
51a. **Soukri, A., A. Mougin, C. Corbier, A. Wonacott, C. Branlant, and G. Branlant.** 1989. Role of the histidine 176 residue in glyceraldehyde-3-phosphate dehydrogenase as probed by site-directed mutagenesis. Biochemistry **28:** 2586–2592.
52. **Stephens, C. M., and R. Bauerle.** 1991. Analysis of the metal requirement of 3-deoxy-D-*arabino*-heptulosonate-7-phosphate synthase from *Escherichia coli*. J. Biol. Chem. **266:**20810–20817.
53. **Veiga-da-Cunha, M., H. Santos, and E. Van Schaftingen.** 1993. Pathway and regulation of erythritol formation in *Leuconostoc oenos*. J. Bacteriol. **175:** 3941–3948.
54. **White, R. S., and W. B. Dempsey.** 1970. Purification and properties of vitamin B_6 kinase from *Escherichia coli*. Biochemistry **9:**4057–4064.
55. **Williams, J. F., P. F. Blackmore, C. C. Duke, and J. K. MacLeod.** 1980. Fact, uncertainty and speculation concerning the biochemistry of D-erythrose-4-phosphate and its metabolic role. Int. J. Biochem. **12:**339–344.
56. **Wincov, I., and L. I. Pizer.** 1974. The mechanism of end product inhibition of serine synthesis. IV. Subunit structure of phosphoglycerate dehydrogenase and steady state kinetic studies of phosphoglycerate oxidation. J. Biol. Chem. **249:**1348–1355.
57. **Woodruff, W. W., III, and R. Wolfenden.** 1979. Inhibition of ribose-5-phosphate isomerase by 4-phosphoerythronate. J. Biol. Chem. **254:**5866–5867.
58. **Zhao, G., and M. E. Winkler.** 1994. An *Escherichia coli* K-12 *tktA tktB* mutant deficient in transketolase activity requires pyridoxine (vitamin B_6) as well as the aromatic amino acids and vitamins for growth. J. Bacteriol. **176:**6134–6138.
59. **Zhao, G., and M. E. Winkler.** 1995. Kinetic limitation and cellular amount of pyridoxine (pyridoxamine) 5′-phosphate oxidase of *Escherichia coli* K-12. J. Bacteriol. **177:**883–891.
60. **Zhao, G., and M. E. Winkler.** 1995. Unpublished results.